Knot physics: Spacetime in co-dimension 2

C. Ellgen*

(Dated: April 28, 2014)

Abstract

Spacetime is assumed to be a branched 4-dimensional manifold embedded in a 6-dimensional Minkowski space. The branches allow quantum interference, each individual branch is a history in the sum-over-histories. A n-manifold embedded in a n+2-space can be knotted. The metric on the spacetime manifold is inherited from the Minkowski space and only allows a particular variety of knots. We show how those knots correspond to the observed particles with corresponding properties. We derive a Lagrangian. The Lagrangian combined with the geometry of the manifold produces gravity, electromagnetism, weak force, and strong force.

*Electronic address: `cellgen@gmail.com`; `www.knotphysics.net`

I. INTRODUCTION

A. Motivation and purpose

Unification of physical laws into a single theory requires a single set of assumptions that generate all observed physical phenomena. Ideally the set of assumptions is simple and the resulting theory contains few independent parameters. To guess the set of assumptions, we consider the assumptions of general relativity, expand the assumptions to increase the explanatory power, and then determine the consequences of that expanded set of assumptions.

General relativity presumes a 4-dimensional Lorentzian manifold and uses a variable metric to explain gravity. Gravity is curvature of the spacetime manifold and particles are a source of that curvature. Perhaps particles have their own inherent spacetime curvature. The equations of general relativity indicate that spacetime curvature propagates dispersively. To prevent that dispersion, we assume that particles are knots in the spacetime manifold. A piecewise linear n-manifold can only be knotted if it is embedded in an n+2-dimensional space [1]. Therefore we assume an embedded 4-dimensional spacetime manifold in a 6-dimensional Minkowski space. To allow quantum interference we extend our assumptions to make it a branched 4-dimensional spacetime manifold. The rest of the paper will develop the idea of a branched 4-dimensional spacetime manifold M, showing how its properties match physical phenomena.

B. Embedded manifolds

Let Λ be an n-dimensional Minkowski space. Then the metric on Λ is a rank 2 tensor of dimension n, $\eta_{\mu\nu} = diag(1, -1, ..., -1)$. The coordinates on Λ are x^ν, where x^ν is an n-dimensional vector. We can embed a manifold Y in Λ. The metric $\bar{\eta}_{\mu\nu}$ on Y is the one inherited from Λ. If Y is a flat m-dimensional subspace spanned by the first m coordinates, then $\bar{\eta}_{\mu\nu} = diag(1, -1, ..., -1, 0, ...0)$ with only the first m diagonal elements non-zero. Curves on Y have length equal to their length in Λ. Tensors on Y have value only on points of Y but the tensors are multilinear functions on the tangent space to Λ. For example, we can define a vector field V^α on Y but the vector field can point in any direction, not just within the tangent space of Y. Differentiation of tensors on Y can be done with ordinary partials. To find the rate of change of a particular tensor one can use the distance as measured in Λ, which is geometrically flat. Let T be some tensor on Y, then we can find the rate of change $\partial_\mu T$ and the rate of change in the direction of a vector v^μ, which is $v^\mu(\partial_\mu T)$. Let $\bar{v}^\mu$ be the projection of v^μ onto Y. Then $v^\mu(\partial_\mu T) = \bar{v}^\mu(\partial_\mu T)$. The rate of change of T in a direction perpendicular to the manifold Y is always zero. Using partial derivatives on Y, we can write the inherited metric $\bar{\eta}_{\mu\nu} = x^\alpha_{\ ,\mu} x_{\alpha,\nu}$.

For an embedded manifold, general covariance need not always apply. We could describe our manifold using a coordinate system that is defined only on the manifold and then general covariance would apply to all of the results that we could derive using that coordinate system. Describing the geometry of knots requires the coordinates of the embedding space and does not allow general covariance.

The spacetime manifold M is a branched 4-dimensional manifold embedded in a 6-dimensional Minkowski space. A spacelike slice of M is a branched 3-manifold in a 5-space. Any 3-manifold can be embedded in a 5-space without self-intersection [8]. Therefore, the dimension of the 6-space does not constrain the homeomorphism class of a spacelike slice of M.

C. Branched manifolds

To allow for quantum properties, we use a branched spacetime manifold. An embedded branched n-manifold is an embedded n-complex such that each point has a well-defined n-dimensional tangent space. In knot physics we use M, a branched 4-manifold embedded in a 6-dimensional Minkowski space. Call B a *branch* of M if B is contained in M and B is a closed unbranched 4-manifold without boundary, see Fig. 1 and Fig. 2. Where distinct branches B_i intersect, the tangent spaces of the branches must be consistent. Each branch is a history in the sum-over-histories path integral. The particles of knot physics are knots. Those knots can take different paths on different branches. When the branches recombine, the geometry of the knots recombines to the average of the knots on each recombining branch. This produces quantum interference. See Fig. 3. Quantum interference will be described to more depth in section VI A.

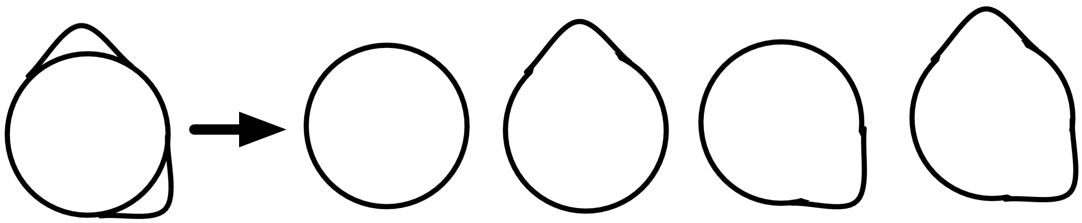

FIG. 1: On the left is a branched 1-manifold Y in a Euclidean 2-space. On the right are the four branches B_i that are contained in Y.

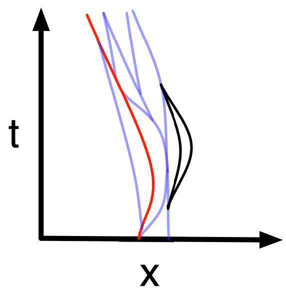

FIG. 2: A branched 1-manifold in a Minkowski 2-space. A branch is highlighted in red. The black piece is not a branch because it has a boundary.

D. Displacement and A^ν

We use a vector field A^ν on our manifold to measure the displacement of the manifold from rest. If the displacement of the manifold is described entirely by its shape then $A^\nu = x^\nu$ everywhere. However, if the manifold has displaced parallel to itself then $A^\nu \neq x^\nu$ somewhere. In this way, even a geometrically flat manifold can be displaced from rest. We require that any displacement must preserve causality. For a constant timelike t_v, a set of constant $A^\nu t_\nu$ separates causal past from causal future. Define

$$A(t_\nu, p) = \{\text{points y sharing a branch with p such that } A^\nu(y)t_\nu = A^\nu(p)t_\nu\}$$
$$I^+(p) = \{\text{points y sharing a branch with p such that } x^\nu(y) - x^\nu(p) \text{ is timelike and future directed}\}$$
$$I^-(p) = \{\text{points y sharing a branch with p such that } x^\nu(y) - x^\nu(p) \text{ is timelike and past directed}\}$$

Then our causality constraint is $A(t_\nu, p) \cap I^-(p) = \emptyset$ and $A(t_\nu, p) \cap I^+(p) = \emptyset$ for all p and all timelike vectors t_ν, see Fig. 4. We further require that $\partial_\nu A^\nu = -2$. Expressing A^ν as a displacement from x^ν of form $A^\nu = x^\nu + \epsilon^\nu$, this gives

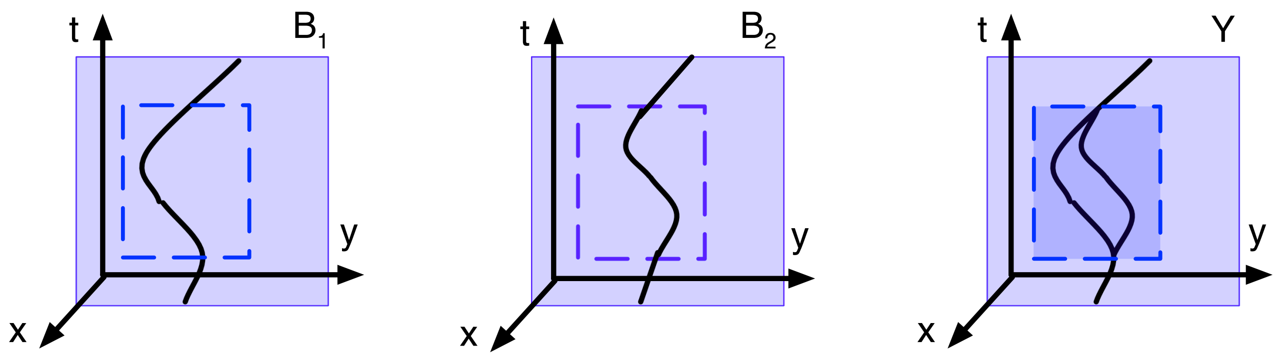

FIG. 3: These are 3 views of a branched 1+1 manifold Y embedded in a Minkowski space. The t coordinate is timelike. The x and y coordinates are spacelike. Y consists of branches B_1 and B_2 shown above. The branches separate on the dotted line. The black curves are the paths of a knot on Y. The knot takes different paths on each branch.

$$\partial_\nu \epsilon^\nu = \partial_\nu (A^\nu - x^\nu) = \partial_\nu A^\nu - \partial_\nu x^\nu = -2 - (-2) = 0 \tag{1}$$

Therefore the displacement $\epsilon^\nu = A^\nu - x^\nu$ satisfies $\partial_\nu \epsilon^\nu = 0$.

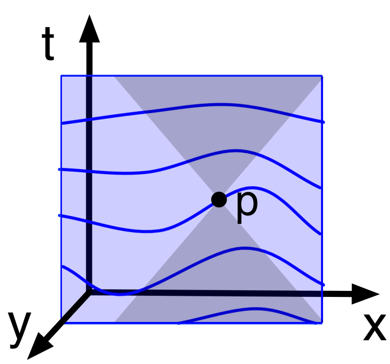

FIG. 4: A branch B in a Minkowski space with timelike coordinate t and spacelike coordinates x and y. The blue curves are sets of constant $A^\nu t_\nu$ for some timelike vector t_ν. The shaded areas are the causal past and the causal future of p. The causality constraint of A^ν requires that the blue curve through p does not intersect the causal past or future of p.

E. A conservation law on M

Without constraint, a branched embedded manifold will tend towards infinite branching and infinite expansion into the co-dimension. To prevent this, we seek a natural tensorial constraint on M.

1. *A conservation law on branching*

The entropy of the spacetime manifold M increases with more branches. If M can branch infinitely, then it will. However, experimental results such as the quantum collapse of state indicate that M does not branch infinitely. To limit the amount of branching, we include a branching conservation law. We describe M as a weighted branched manifold. We begin by assuming a piecewise-constant weight function w on M. Then every point on M has some weight w and the weight changes only where branches separate. The weight on the separated branches adds up to the weight of the unseparated branch. If we require that each $w_i \geq 1$ then M can branch only a finite number of times. See Fig. 5.

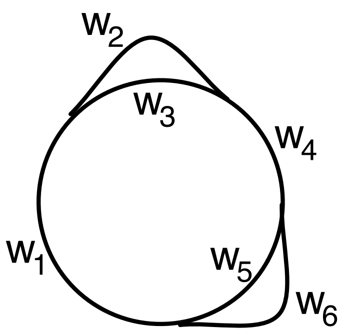

FIG. 5: A weighted branched 1-manifold. The weights w_i are additive such that $w_1 = w_2 + w_3 = w_4 = w_5 + w_6$.

2. *A conservation law on individual branches*

The entropy of M also depends on individual branches. Allowing a branch to expand into the co-dimension can increase its entropy. Without a constraint on the size, a branch will entropically tend to expand infinitely into the co-dimension. Likewise, if there is no bound on the curvature of a branch's geometry or A^ν field, then the curvature tends entropically towards infinite curvature. We use the A^ν vector field to describe a metric on M, $h_{\mu\nu} = A_{\alpha,\mu}A^{\alpha}{}_{,\nu}$. Let $\dot{R}^{\mu\nu}$ be the Ricci curvature based on $h_{\mu\nu}$. Then we require $\dot{R}^{\mu\nu} = 0$. With $\partial_\nu A^\nu = -2$, the requirement $\dot{R}^{\mu\nu} = 0$ also constrains the expansion into the co-dimension.

3. *A combined conservation law*

We have a constraint on branching ($w_i \geq 1$) and a constraint on geometry ($\dot{R}^{\mu\nu} = 0$). We can combine the two into a single constraint. We assume a conformal factor ρ and a weight

$w \geq 1$. The weight w is piecewise-continuous and differentiable with discontinuities only where M branches. At branch separations, w and all derivatives of w are additive like a branch weight. Now we make a new metric $g_{\mu\nu} = \rho^2 h_{\mu\nu} = \rho^2 A_{\alpha,\mu} A^{\alpha}{}_{,\nu}$. Let $\hat{R}^{\mu\nu}$ be the Ricci curvature based on $g_{\mu\nu}$. We require that $\hat{R}^{\mu\nu} = 0$. From the volume preservation property of Ricci flatness, the volume of splitting branches must be conserved, therefore the conserved branch weight must be $w = (-det(g))^{1/2}$ (here $g_{\mu\nu}$ is considered as a 4×4 matrix in its tangent space). For $A^{\nu} \approx x^{\nu}$ we have $w \approx \rho^4$. These constraints allow a trade between the size of the branches and the number of branches. See Fig. 6.

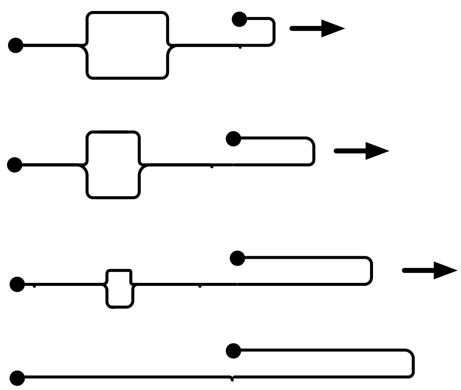

FIG. 6: This is a sequence of spacelike slices of a 1+1 manifold. It is being pulled on the right side. As the right side extends, the weight w reduces. The constraint $w \geq 1$ pulls on the branches, shrinking them. Eventually the branches recombine.

II. ASSUMPTIONS

The assumptions are the following:

- **We assume a Minkowski 6-space** Ω**.** The metric on Ω is $\eta_{\mu\nu} = diag(1, -1, -1, -1, -1, -1)$. The coordinates are x^ν.
- **We assume a branched 4-manifold** M **embedded in** Ω**.** A *branch* of M is any closed unbranched 4-manifold B without boundary that is contained in M. The metric $\bar{\eta}_{\mu\nu}$ on M is inherited from Ω. For convenience of coordinates we assume that, if M is flat, then M is in the subspace spanned by x_0, x_1, x_2, x_3.
- **We assume that no branch of** M **can intersect itself.** This is necessary to prevent knots from spontaneously untying.
- **We assume a vector field** A^ν **that describes the displacement of** M **and** A^ν **preserves causality. The field satisfies** $\partial_\nu A^\nu = -2$**.** If there is no parallel displacement then $A^\nu = x^\nu$, the field is equal to the coordinate.
- **Let** ρ **be a piecewise-continuous scalar on** M**. Define the metric** $g_{\mu\nu} = \rho^2 A_{\alpha,\mu} A^{\alpha}{}_{,\nu}$**. We assume the Ricci curvature based on** $g_{\mu\nu}$ **satisfies** $\hat{R}^{\mu\nu} = 0$**.** This implies that $w = (-det(g))^{1/2}$ is the conserved branch weight. For $A^\nu \approx x^\nu$ we have $w \approx \rho^4$.

III. THE LAGRANGIAN

The behavior of the interacting branches of M produces quantum physics. The aggregate behavior of the branches of M produces classical physics. To describe the relation between the quantum and classical descriptions we find a Lagrangian L that describes the most probable branch. Then we find a manifold Φ_M that optimizes the Lagrangian L. The aggregate behavior of the branches of M will cluster around Φ_M.

A. Ricci flat solutions for photons and gravitons

Waves in A^ν or manifold geometry are consistent with Ricci flatness. However, the branch weight w allows for additional solutions. The wave equation requires that waves propagate on spherical wave fronts. Using w to compensate the geometry of the A^ν field, one can have a wave with finite effective width. In directions perpendicular to the wave vector k^ν, the A^ν field does not satisfy the wave equation but, including w, the metric does satisfy $\hat{R}^{\mu\nu} = 0$. The result is a wave of finite width that has properties of both particles and waves.

The Ricci flat solution for photons and gravitons can appear and disappear spontaneously, corresponding to virtual photons and virtual gravitons. Because these virtual particles are under-constrained by $\hat{R}^{\mu\nu} = 0$, they maximize entropy. Entropy maximization determines the behavior of fields on M, which we describe using a Lagrangian.

B. Collapse of state

The probability of an event is proportional to the number of branches that include that event. Recombination and separation increase the number of branches, see Fig. 7. Recombination and separation happen when branches are close. Therefore probability is optimized when branches stay close to each other. Assume there are two possible paths for the space-time manifold that become increasingly different over time. To optimize probability, the branches of M follow one path or the other and the number of branches close to the other path goes to zero. This is a collapse of state, see Fig. 8.

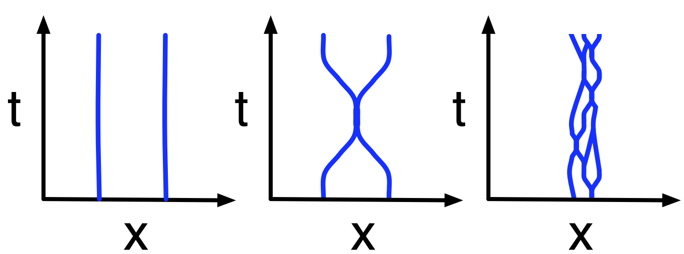

FIG. 7: On the left there are two branches. In the middle there are 4 branches: left-left, left-right, right-left, and right-right. Therefore branches tend to stay close to optimize probability, as on the right.

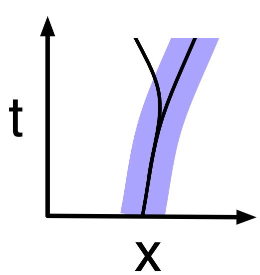

FIG. 8: The blue line represents the branches of a branched 0+1-manifold. The black lines are two possible paths the branched manifold can follow. As the paths diverge, the state of the branched manifold collapses to one of the paths.

C. The Lagrangian

The branches of M stay close to each other to maximize recombination. However, M is still under-constrained, so we expect the aggregate behavior of the branches to maximize entropy. Let Φ_M be an unbranched manifold such that M maximizes its entropy when its branches are close to Φ_M. We assume that Φ_M has a A^ν displacement vector field with $\partial_\nu A^\nu = -2$ and metric $g_{\mu\nu} = \rho^2 A_{\alpha,\mu} A^\alpha{}_{,\nu}$. Constrain Φ_M such that the Ricci tensor $\hat{R}^{\mu\nu}$ based on $g_{\mu\nu}$ satisfies $\hat{R}^{\mu\nu} = 0$ and $w = (-det(g))^{1/2} \geq 1$. We begin with the unbranched manifold Φ_M and then make M from it by separating Φ_M into branches in a way that conserves w.

The entropy is maximal when the manifold is far from the causality constraint on A^ν. For $F^{\mu\nu} = A^{\nu,\mu} - A^{\mu,\nu}$, the causality constraint is equivalent to $F^{\mu\nu} F_{\mu\nu} \geq -2$. The entropy is maximized when $F^{\mu\nu} F_{\mu\nu}$ is maximal. If only the field $F^{\mu\nu}$ can vary, then the Lagrangian is $L_F = w \ln(1 + (1/2) F^{\mu\nu} F_{\mu\nu}) \approx w(1/2) F^{\mu\nu} F_{\mu\nu}$. (See section VII A.)

Likewise, the scalar curvature R with respect to the inherited metric $\bar{\eta}^{\mu\nu}$ affects the entropy of M. The w-weighted volume of M is conserved by $\hat{R}^{\mu\nu} = 0$. Stretching M by increasing its scalar curvature reduces the value of w, which reduces the number of times that M can branch. The entropy of M increases as the number of branches increases. The value of w is maximized by minimizing the volume $dV \approx (1 + R) dV_{flat}$. If only the curvature can vary, then the Lagrangian is $L_R = w/(1 + R)$, or the approximately equivalent $L_R \approx -wR$. (See section VII B.)

Allowing both $F^{\mu\nu}$ and R to vary, the Lagrangian is

$$L = w(1/2) F^{\mu\nu} F_{\mu\nu} - wR = w\big((1/2) F^{\mu\nu} F_{\mu\nu} - R\big) \tag{2}$$

Let Φ_M be a manifold that optimizes the action $S[\Phi_M] = \int w\big((1/2) F^{\mu\nu} F_{\mu\nu} - R\big) d\Phi_M$. Then M maximizes its entropy by being close to Φ_M. Assuming w is approximately constant, we have the term $(1/2) F^{\mu\nu} F_{\mu\nu}$ that is the Lagrangian of electromagnetism and the scalar curvature R from general relativity.

D. Energy-momentum tensor

We use the action $S[\Phi_M] = \int w\big((1/2) F^{\mu\nu} F_{\mu\nu} - R\big) d\Phi_M$ to get the energy-momentum tensor. The measure $d\Phi_M$ scales by $1/\gamma = (1 - \beta^2)^{1/2}$ when the manifold is in motion.

We include $1/\gamma$ in the energy-momentum tensor. How does the energy-momentum tensor transform in motion? Assume at rest $T^{\mu\nu}_r = E\bar{\eta}^{\mu\nu}$. At rest $\bar{\eta}^{\mu\nu} = diag(1, -1, -1, -1, 0, 0)$. To find $T^{\mu\nu}$ for the manifold in motion, we Lorentz transform $\bar{\eta}^{\mu\nu}$. If the manifold is in motion with velocity $\vec{\beta} = (1, 0, 0, 0, -\beta, 0)$ then

$$T^{\mu\nu} dM = \frac{E}{\gamma} \begin{bmatrix} \gamma^2 & 0 & 0 & 0 & \beta\gamma^2 & 0 \\ 0 & -1 & 0 & 0 & 0 & 0 \\ 0 & 0 & -1 & 0 & 0 & 0 \\ 0 & 0 & 0 & -1 & 0 & 0 \\ \beta\gamma^2 & 0 & 0 & 0 & \beta^2\gamma^2 & 0 \\ 0 & 0 & 0 & 0 & 0 & 0 \end{bmatrix} dtdV. \tag{3}$$

For a volume dV of spacetime, the energy is $\gamma E dV$ and the momentum is $\beta\gamma E dV$ in the direction of motion. This happens whenever the direction of motion is not in the tangent space at dV. Particles have rest mass because the tangent space of the knot is not parallel to flat spacetime.

IV. TOPOLOGY CHANGE ON M

We assume that particles are knots on M. When particle pairs are created, the spacelike slice of M changes topology. The spacetime manifold M is embedded in a Minkowski space and M has finite energy. Finite energy constrains the topology changes of spacelike slices of M, which limits the possible particle topologies.

A. Lorentzian cobordism

If M is everywhere Lorentzian then the topology change on M must occur by Lorentzian cobordism. However, a Lorentzian cobordism does not allow topology change.

A *cobordism* is a triple (W, A, B) with A and B n-1-dimensional manifolds and W a n-dimensional manifold such that the boundary of W is the disjoint union $A \sqcup B$. A *Lorentzian cobordism* is a cobordism such that W is Lorentzian and the boundary of W is the disjoint union $A \sqcup B$ with A and B spacelike.

Results from Geroch [9] show that a Lorentzian cobordism on M must also be a diffeomorphism, which means there is no topology change. For a n-manifold X, the metric signature is (i_+, i_0, i_-), with i_+ the positive eigenvalues, i_0 the zero eigenvalues, and i_- the negative eigenvalues. If X is Lorentzian then the metric signature is $(1, 0, n-1)$. Let K be a spacelike slice of M. Assume M has metric signature $(1, 0, 3)$ everywhere. There is always a timelike vector field orthogonal to K and everywhere non-zero. Using that timelike vector field we can generate a new surface K' contained in M that is some infinitesimal distance from K either into the future or the past. The surface K' is isotopic to K, therefore metric signature $(1, 0, 3)$ in the neighborhood of K implies that the manifold changes only by isotopy in a neighborhood of K. (This is the essence of the proof by Geroch.) To allow a non-isotopy embedding, M must have a metric signature other than $(1, 0, 3)$ somewhere.

B. Finite energy embedding

The energy of a 3-volume dV in motion with magnitude of velocity β is proportional to γdV, where $\gamma = (1 - \beta^2)^{-1/2}$. If M has finite energy then β must be less than 1 everywhere *except a set of measure zero*. On that set of measure zero, the inherited metric $\bar{\eta}_{\mu\nu}$ can be degenerate, which means that M is not Lorentzian.

Let X be a finite energy embedding. Then, on a set of measure zero, X can have a lightlike vector instead of a timelike vector, giving metric signature $(0, 1, n-1)$ or $(0, 2, n-2)$. Likewise, the metric $g_{\mu\nu} = \rho^2 A_{\alpha,\mu} A^{\alpha}{}_{,\nu}$ can be degenerate if A^ν is at its causal limit. In that case, the metric signature of $g_{\mu\nu}$ can be $(0, 2, n-2)$. Because $A^{0,\mu}$ is a causal vector field wherever $A^{0,\mu}$ is timelike, the vector field $A^{0,\mu}$ must be lightlike at every topology change.

A finite energy embedding of M has metric signature $(1, 0, 3)$ almost everywhere, signature $(0, 1, 3)$ or $(0, 2, 2)$ on at most a set of measure zero, and all other signatures nowhere. If the manifold has metric signature $(0, 2, 2)$ somewhere then we say that manifold is *kinked* at that point. Finite energy embeddings are less constrained than Lorentzian cobordisms and we will see how they allow for topology change on M.

C. An example topology change

We consider an example manifold X embedded in a Minkowski space and demonstrate how X can change topology with a finite energy embedding. Let a spacelike slice of X be an infinite strip $\mathbb{R} \times I$ for an interval I. Then we can let X move such that two intervals on X are on the light cone. The metric is degenerate on those intervals. On a spacelike slice, those intervals contract to points. This allows X to twist at each of those points. When the velocity reduces such that the intervals are no longer degenerate, X has a twist, which is a change in its topology, see Fig. 9. Though M has more dimensions than X, the topology changes on M are not much more than twists.

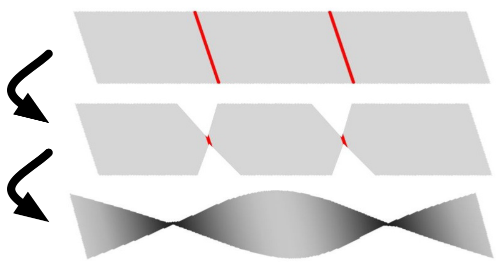

FIG. 9: Let an infinite strip $\mathbb{R} \times I$ move so that two intervals are Lorentz contracted to points. Twist around those points. The result is a twist in the strip.

D. Homology

Let B be a branch of the spacetime manifold M. Let K be a spacelike slice of B. The manifold B is a finite energy embedding, which constrains the homology group $H_0(K)$ and homotopy groups $\pi_1(K)$ and $\pi_2(K)$.

1. $H_0(K)$

The $rank(H_0(K)) = 1$ (proof in section VII C 1). This implies that the universe cannot split off separate pieces and cannot connect with other pieces.

2. $\pi_1(K)$

$\pi_1(K)$ must be finite (proof in section VII C 2). Therefore there are no handles on K.

3. $\pi_2(K)$

If the topology of K is a non-trivial embedding then $\pi_2(K)$ must be non-trivial (proof in section VII C 3).

V. PARTICLES

We describe the topology of particles on the manifold using connected sums. If a spacelike slice contains no particles then that spacelike slice has topology $\mathbb{R}^3$. If a spacelike slice has one particle with some topology labeled T_P, then the total slice has topology $\mathbb{R}^3 \# T_P$ where $\#$ denotes the connected sum, presuming that the form of the connected sum has been specified. We discuss the topology of particles on the manifold as if the rest of the universe were topologically trivial, implicitly assuming that the topology of the rest of the universe is not relevant to the discussion.

A. Rest mass and orientability

The description of rest mass in section III D shows that a particle whose tangent space is not parallel to flat spacetime has rest mass. Therefore, any particle with non-trivial topology has rest mass. We therefore consider only particles with rest mass when describing particle topology. Specifically, we describe the topology of the elementary fermions.

Fermion spin-statistics suggest that fermions are non-orientable. A coordinate frame on an orientable spacetime manifold uses $SO(3,1)$ as its rotation group. However, fermions use the group $Spin(3,1)$, the group associated with non-orientable topologies. We therefore consider non-orientable topologies when describing fermions.

B. $S^1 \times P^2$

To describe elementary fermions we need a non-orientable topology. Using the Lickorish-Wallace theorem [10–12] we know that every closed, connected, non-orientable 3-manifold is obtained by Dehn surgery on a link in the non-orientable 2-sphere bundle over the circle. We show that the topology $\mathbb{R}^3 \#(S^1 \times P^2)$ can describe leptons and quarks. Proving that no other topology would suffice is a subject for future work. For convenience we will sometimes refer to the topology $\mathbb{R}^3\#(S^1 \times P^2)$ as $S^1 \times P^2$. Single $S^1 \times P^2$ are leptons. Linked $S^1 \times P^2$ are quarks.

To make the connected sum $\mathbb{R}^3\#(S^1 \times P^2)$ we first make the connected sum $\mathbb{R}^2\#P^2$. We begin with $\mathbb{R}^2$ in polar coordinates, written (r, θ). Now we cut out a unit disk to make $\mathbb{R}^2 - D^2$ leaving points (r, θ) with $r \geq 1$. With that set we make the following mapping:

$$X : (r, \theta) \to (g(r), \theta, h(r)sin(2\theta), h(r)cos(2\theta)) \tag{4}$$

$$g(r) = \begin{cases} 2r - 2 & \text{if } r < 2 \\ r & \text{otherwise} \end{cases} \qquad h(r) = \begin{cases} 2 - r & \text{if } r < 2 \\ 0 & \text{otherwise} \end{cases}$$

We are taking $\mathbb{R}^2 - D^2$, stretching the annulus $1 \leq r \leq 2$ to cover the missing disk, and then identifying opposite points of the boundary on a circle in the x_3, x_4 coordinates, see Fig. 10.

To make the connected sum $\mathbb{R}^3\#(S^1 \times P^2)$, we fiber over the circle. Let C be a circle of radius R in $\mathbb{R}^3$ and use polar coordinates (r, θ) to describe the plane that is perpendicular to a point on C. Let ϕ describe the angular coordinate of the point on C. Then every point on $\mathbb{R}^3$ is at coordinates (r, θ, ϕ). Let T be the solid torus $r < 1$. Remove the solid torus T from $\mathbb{R}^3$ leaving $\mathbb{R}^3 - T$, which is points of the form (r, θ, ϕ) and $r \geq 1$. We map:

$$X : (r, \theta, \phi) \to (g(r), \theta, \phi, h(r)sin(2\theta), h(r)cos(2\theta)) \tag{5}$$

$$g(r) = \begin{cases} 2r - 2 & \text{if } r < 2 \\ r & \text{otherwise} \end{cases} \qquad h(r) = \begin{cases} 2 - r & \text{if } r < 2 \\ 0 & \text{otherwise} \end{cases}$$

This is a fibering of the previous mapping over a circle. We note that there are other possibilities for the fibering. Specifically, a type-n mapping of the form

$$X : (r, \theta, \phi) \to (g(r), \theta, \phi, h(r)sin(2\theta + n\phi), h(r)cos(2\theta + n\phi)) \tag{6}$$

where n is any integer. When referring to a $S^1 \times P^2$ with a type-n mapping, we call it a $(S^1 \times P^2)_n$. We note that our homology constraints are satisfied for $(S^1 \times P^2)_n$ for all n.

C. Finite energy embedding pair creation for $S^1 \times P^2$

To demonstrate that a finite energy embedding allows creation of pairs of $S^1 \times P^2$, we can likewise show pair annihilation. Pair creation is the same process in reverse. To annihilate

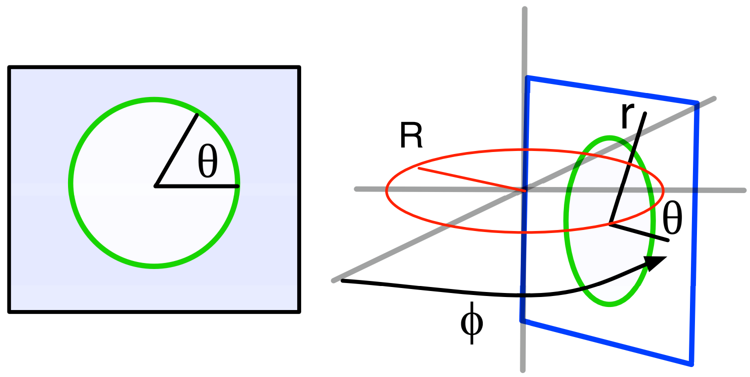

FIG. 10: On the left is $\mathbb{R}^2 - D^2$ in polar coordinates. On the right is $\mathbb{R}^3 - T$, with a slice at $\phi = \phi_0$. Identifying opposite points on the circumference of the green circle makes $\mathbb{R}^2\#P^2$ and $\mathbb{R}^3\#(S^1 \times P^2)$, respectively.

a pair of $S^1 \times P^2$, we require that they are both $(S^1 \times P^2)_n$ with the same value of n. We demonstrate annihilation of pairs of P^2 on a 2-manifold and fiber that annihilation over the circle to annihilate each $(S^1 \times P^2)_n$.

We begin with $\mathbb{R}^2\#P^2\#P^2$ and annihilate the pairs of P^2 by bringing the two P^2 adjacent to each other, closing the distance. To make point identifications between the two, we use the degenerate metric. When the points are identified, the $\mathbb{R}^2\#P^2\#P^2$ becomes $\mathbb{R}^2\#S^2 = \mathbb{R}^2$, which is annihilation, see Fig. 11.

However, the A^ν field must also be degenerate at the transition. Specifically, the vector field $A^{0,\mu}$ must be lightlike at the transition. Therefore one P^2 must have A^0 field at higher value than the other. Likewise, in pair creation, when a pair of $S^1 \times P^2$ are created, one of them will have higher A^0 field value than the other. Therefore, at least one particle must be charged at the pair creation. Additional discussion of charge is available in [14].

D. Quarks, linked $S^1 \times P^2$

Linked $S^1 \times P^2$ are quarks. A pair $\mathbb{R}^3\#(S^1 \times P^2)\#(S^1 \times P^2)$ can link as an embedding in $\mathbb{R}^5$. To demonstrate that, we link a pair $\mathbb{R}^2\#P^2\#P^2$ embedded in 4 dimensions and then fiber that link over S^1.

To link a pair of the form $\mathbb{R}^2\#P^2\#P^2$, begin with a disk D^2 embedded in $\mathbb{R}^4$ and attach a P^2 to make $D^2\#P^2$. This is topologically equivalent to a D^2, but for the moment we will

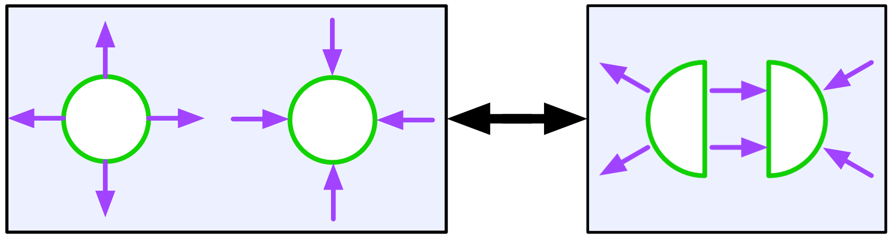

FIG. 11: We bring together two P^2 to annihilate. The purple arrows indicate the spacelike components of $A^{0,\mu}$. If the metric becomes degenerate on the piece of the manifold between the two P^2 then the pair of P^2 become an S^2, which means the pair annihilate.

preserve its geometry. Now take the product $(D^2\#P^2)\times I$ for a unit interval $I=[0,1]$, again as an embedding in $\mathbb{R}^4$. Take the outer edge $(D^2\#P^2)\times\{0,1\}$. Perform surgery on the boundary to make one boundary that is a S^1, call the result L. Glue the boundary of L to the boundary of $\mathbb{R}^2-D^2$. The result is a linked pair of P^2 on $\mathbb{R}^2$ embedded in $\mathbb{R}^4$. See Fig. 13. To link more copies of P^2, select more points from the interval, as in $(D^2\#P^2)\times\{0,1/n,2/n,...1\}$. This linking extends to linked $S^1\times P^2$ by fibering over S^1.

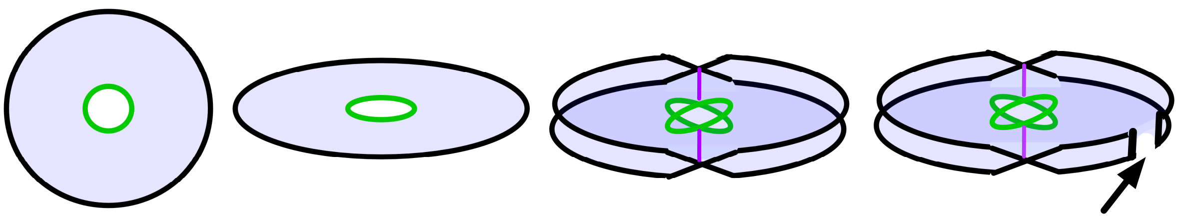

FIG. 12: Let the circle with the green inner circle denote a $D^2\#P^2$. Tilt it backward, to change the view. Take the product $(D^2\#P^2)\times\{0,1\}$. The top left side of the diagram connects to the lower right side and vice versa. In 3 dimensions the two sides intersect in the middle, denoted by the purple line. In 4 dimensions there is no intersection. Perform surgery on the boundary, as marked by the arrow, to make L.

To see that the $\mathbb{R}^2\#P^2\#P^2$ pair is linked, project the embedding into 3 dimensions. In every projection, the pair must intersect in a crossing, which implies linking. That crossing is always a non-trivial element of the $\mathbb{R}^2\#P^2$ homology. Assume that 3 copies of P^2 are linked, label them A,B,C. If A and B are linked then any projection and any embedding will produce a AB crossing on B that is a non-trivial element of the homology of B. The same is true for the BC crossing. Therefore the AB crossing must intersect the BC crossing

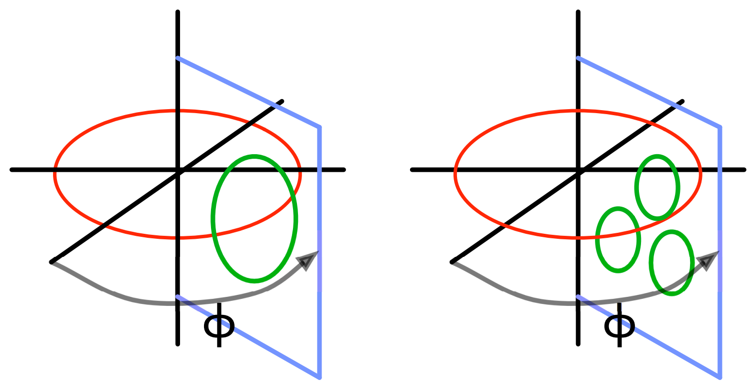

FIG. 13: Linked $\mathbb{R}^3\#(S^1 \times P^2)$ are linked $\mathbb{R}^2\#P^2$ fibered over a circle

in any projection and any embedding. This implies that A and C are also linked. Therefore, for n linked copies of P^2, if A is linked to B and B is linked to C then A is linked to C; the linking property is transitive among all links. This also extends to $S^1 \times P^2$.

For two linked $(S^1 \times P^2)_n$ that have the same value of n and opposite charge, the pair can annihilate. However, for three $S^1 \times P^2$, annihilation of any two with each other is impossible because the annihilation would pass through intersection with the third quark.

E. Quantum phase factor

Beginning with the mapping $X : (r, \theta, \phi) \to (g(r), \theta, \phi, h(r)sin(2\theta + n\phi), h(r)cos(2\theta + n\phi))$ we see an allowed rotation in the x_4, x_5 coordinates. The rotation adds a ωt factor of the form

$$X : (r, \theta, \phi) \to (g(r), \theta, \phi, h(r)sin(2\theta + n\phi + \omega t), h(r)cos(2\theta + n\phi + \omega t)) \tag{7}$$

This rotation improves of the action of the Lagrangian and therefore occurs in every $S^1 \times P^2$. We later show that this rotation is the quantum phase factor of the particle.

F. Generations

Elementary fermions have multiple generations. The generations correspond to the integer n in the topology $(S^1 \times P^2)_n$. A $(S^1 \times P^2)_n$ has the same homeomorphism class as a $(S^1 \times P^2)_m$ for any values of m and n. However, we prove in section VII D that the embedding class of $(S^1 \times P^2)_m$ and $(S^1 \times P^2)_n$ are different if $m \neq n$. By the constraints of M, they are therefore topologically distinct.

1. Generation transitions

On an uncharged $S^1 \times P^2$ there is a finite energy topological transition between $(S^1 \times P^2)_m$ and $(S^1 \times P^2)_n$ with $m \neq n$. An intermediate state in the transition is the mapping

$$X : (r, \theta, \phi) \rightarrow (g(r), \theta, \phi, h(r,\phi)sin(2\theta + n\phi), h(r,\phi)cos(2\theta + n\phi))$$
$$g(r) = \begin{cases} 2r - 2 & \text{if } r < 2 \\ r & \text{otherwise} \end{cases} \qquad h(r,\phi) = \begin{cases} |sin(\phi/2)|(2-r) & \text{if } r < 2 \\ 0 & \text{otherwise} \end{cases} \tag{8}$$

We have chosen $h(r, \phi)$ so that one P^2 slice out of the $S^1 \times P^2$ contracts to a point, call this a *P-contraction*. The manifold is kinked at that point. Call that intermediate state $(S^1 \times P^2)*$. The $(S^1 \times P^2)*$ can twist around the kink so that a $(S^1 \times P^2)_m$ twists until it is a $(S^1 \times P^2)_n$ with $m \neq n$.

2. Charged generation transition obstruction

When a $S^1 \times P^2$ changes generation it passes through the $(S^1 \times P^2)*$ configuration. If the $S^1 \times P^2$ is charged then all the charge at the P-contraction is at a single point. Instead the $S^1 \times P^2$ passes the charge to another particle so that it can decay without charge.

3. Linked charged generation transition

Linked generation transitions introduce a complication. A $(S^1 \times P^2)*$ that is linked to a $S^1 \times P^2$ would intersect at the P-contraction. To prevent that intersection, all of the linked $S^1 \times P^2$ must P-contract together so that each of them is a $(S^1 \times P^2)*$ and the point of the P-contraction is the same point for all of them.

G. Particle generation limits

We have shown how the $S^1 \times P^2$ topology can describe the elementary fermions. The difference between generations can be explained using different values of n for $(S^1 \times P^2)_n$.

For charged fermions, only 3 generations have been observed, which are $n = 0, 1, 2$. Perhaps higher generations of charged fermions are constrained by energy and stability.

For neutrinos, there have also been only 3 generations observed, which may be due to the rate of generation transition. Neutrinos are unlinked uncharged $S^1 \times P^2$, there is no obstruction to their generation transition. If we estimate a neutrino mass around 0.1eV, then the spin angular momentum gives a S^1 radius for a neutrino of about $10^{-5}m$, which is significantly larger than the other particles. Based on the mass estimate, the oscillations for neutrinos between generation 2 and 3 (which is between $(S^1 \times P^2)_1$ and $(S^1 \times P^2)_2$) occur in about $10^{-12}s$ in the rest frame of the neutrino. For faster oscillations, the frequency would be faster than the time required for light to travel from one side of the neutrino to the other, which implies that the neutrino mass would never equilibrate. We therefore expect 3 distinguishable generations of neutrino masses corresponding to $(S^1 \times P^2)_0$, $(S^1 \times P^2)_1$, and $(S^1 \times P^2)_n$ for $n \geq 2$.

H. Particle summary

Table I summarizes the classification of elementary fermions. All elementary fermions are of type $S^1 \times P^2$. For each type the $S^1 \times P^2$ can be uncharged, charged, or charged and linked. If the $S^1 \times P^2$ is charged and linked it is a quark. Additional discussion of particle geometry, size, angular momentum, charge, and fractonal quark charge is in [14].

TABLE I: The elementary fermions

	$(S^1 \times P^2)_0$	$(S^1 \times P^2)_1$	$(S^1 \times P^2)_2$
uncharged	ν_e	ν_μ	ν_τ
charged	e	μ	τ
charged, linked, 2/3	u	c	t
charged, linked, 1/3	d	s	b

VI. QUANTUM MECHANICS AND FIELDS

A. Quantum wave functions

On a branched manifold, a knot may take many different paths to go from one point in spacetime to another. The probability of a knot that starts at point A arriving at point B is the sum over all branches such that the knot begins at A and ends at B. At a transition such that the knot is on m incoming branches and n outgoing branches, each incoming branch can be matched to an outgoing branch. The probability of the transition is therefore proportional to $P = mn$. See Fig. 14.

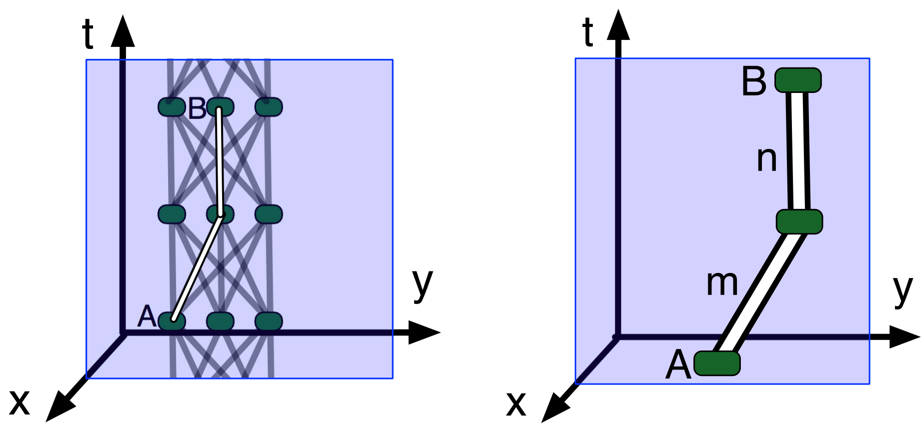

FIG. 14: Assume that branches only recombine at a discrete set of times and knots only follow a discrete set of paths. On the left is the branched manifold with knot paths in gray and points of knot recombination in green. One path from A to B is highlighted. On the right, the path is shown separately. The transition has m incoming branches and n outgoing branches. The probability of the transition is proportional to the number of combinations, $P = mn$.

A knot has a mapping $X(Ke^{i\theta_j})$ of the following form:

$$X(Ke^{i\theta_j}) : (r, \theta, \phi) \rightarrow (g(r), \theta, \phi, Kh(r)sin(2\theta + \theta_j), Kh(r)cos(2\theta + \theta_j))$$
$$g(r) = \begin{cases} 2r - 2 & \text{if } r < 2 \\ r & \text{otherwise} \end{cases} \qquad h(r) = \begin{cases} 2 - r & \text{if } r < 2 \\ 0 & \text{otherwise} \end{cases} \tag{9}$$

The manifold branches as often as possible and there are branches with mappings $X(Ke^{i\theta_j})$ with $0 < K \leq K_j$ for some maximum amplitude K_j. See Fig. 15. The quantum amplitude can be written using a complex number $\psi_j = K_j e^{i\theta_j}$.

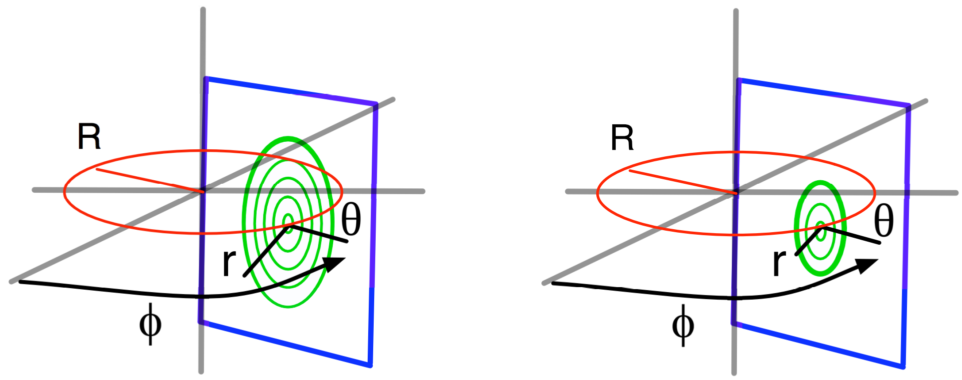

FIG. 15: For a knot with maximum amplitude K_j and angle θ_j, the manifold branches have mappings $X(Ke^{i\theta_j})$, such that $0 < K \leq K_j$. This is loosely illustrated by the diagram for two different maximum amplitudes. Each green circle indicates a $S^1 \times P^2$ of that amplitude.

We separate the branches of M into collections C_j, separated according to particle location. The branches of a collection C_j have geometry of the form $X(Ke^{i\theta_j})$, for $0 < K \leq K_j$. For each C_j the quantum amplitude is $\psi_j = K_j e^{i\theta_j}$ at the knot location and $\psi_j = 0$ everywhere else. We put the branches from each C_j together on Φ_M into a single quantum amplitude $\psi(x) = \sum_j \psi_j(x)$. See Fig. 16. A measurement of knot location has an equal number of incoming and outgoing branches and is proportional to $P(x) = \sum_j |\psi_j(x)|^2$. For any x, at most one $\psi_j(x)$ is nonzero, therefore $P(x) = \sum_j |\psi_j(x)|^2 = |\psi(x)|^2$.

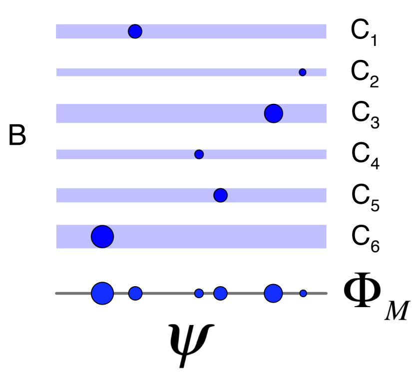

FIG. 16: Branches B of M separated into collections C_j where each collection has a different location for the particle, indicated by the blue circles. The number of branches is indicated by the thickness of the C_j line. The ψ_j are collected into one function $\psi = \sum_j \psi_j$ on Φ_M at the bottom.

When branches of M recombine, they recombine to the w-weighted average. For waves like photons and gravitons, this implies the wave amplitudes add according to their phase.

For fermions, the w-weighted average depends on their geometry $X(Ke^{i\theta})$ and the weight w. The amplitude K affects weighted average because greater extension into the co-dimension will have greater effect on recombination. The geometric effect of K is linear in K. However, the amplitude also affects the weight w because of Ricci flatness, $\hat{R}^{\mu\nu} = 0$. The weight is $w \approx \rho^4$. If the manifold is in motion relative to the rest frame, this becomes $w \approx \rho^4/\gamma$. From [14] we see that γ and the conformal factor ρ depend on K such that $\rho \propto 1/K$ and $\gamma = \rho^2$. Then we have $w \approx \rho^4/\gamma = \rho^2 \propto 1/K^2$. The geometric volume of the branch is linear in the amplitude K, therefore the integrated weight over the volume is $\int(w/\gamma)dV \propto 1/K$. Then the effect on geometry including the effect of extension into the co-dimension is $K\int(w/\gamma)dV \propto 1$. Therefore, the amplitude of an individual branch does not affect its contribution to the w-weighted average. The effect of particle amplitude on recombination is due only to the number of branches that fit within the maximum amplitude K_j, which is linear in K_j. Therefore, the wave function for the recombined geometry of multiple C_j is $\psi_{sum} = \sum_j \psi_j$. The maximum amplitude branch has amplitude $|\psi_{sum}|$, which determines the number of branches that fit within the recombined geometry, which determines the probability.

Let q represent the ψ function of every particle type and let H be the Hamiltonian. Then we use a path integral to describe transition probabilities.

$$\langle q_N|e^{-iHT}|q_1\rangle = (\prod_j \int dq_j)\langle q_N|e^{-iH\Delta t}|q_{N-1}\rangle ... \langle q_2|e^{-iH\Delta t}|q_1\rangle \tag{10}$$

It remains to show that the Hamiltonian corresponding to the action $S[\Phi_M] = \int w\big((1/2)F^{\mu\nu}F_{\mu\nu} - R\big)d\Phi_M$ produces results that match experiment. For that purpose, we need to show that the action at least can produce the fundamental interactions: electromagnetism, weak force, strong force, and gravity.

B. Electromagnetism

For constant w, the action $S[\Phi_M] = \int w\big((1/2)F^{\mu\nu}F_{\mu\nu} - R\big)d\Phi_M$ includes the term $(1/2)F^{\mu\nu}F_{\mu\nu}$. This is the Lagrangian of electromagnetism. On flat space $F^{\mu\nu}F_{\mu\nu}$ is a massless field. The action of the gauge group $SO(2)$ (isomorphic to $U(1)$) on x_4, x_5 has no effect on the electromagnetic field. Charge is described in [14].

C. Electroweak force

If the manifold is not flat, then the velocity of a Lorentz transformation may not be in the tangent space. From section III D, that implies the energy Lorentz transforms with rest mass. Then $F^{\mu\nu}$ field energy also transforms with rest mass. When a particle is accelerated, for example in particle collision, its geometry responds elastically. If the elastic response is confined to the particle, this is a virtual Higgs boson. If the elastic response produces a transverse wave on spacetime, the wave spontaneously decays to other particles. This is a real Higgs boson.

With a non-constant tangent space, there are still field components that are unaffected by the action of $SO(2) \cong U(1)$ on x_4, x_5. However, there are other field components that are perpendicular to x_1, x_2, x_3. The timelike component x_0 is never perpendicular, the manifold always has a timelike tangent vector. For field components perpendicular to x_1, x_2, x_3 we use the gauge group $SO(3)$. However, fermions are non-orientable and there is no consistent orientation for the rotational group associated with the tangent space to the manifold. To correct that we use $SU(2)$, the double cover of $SO(3)$. The gauge group is therefore $U(1) \times SU(2)$.

Far from particles the spacetime manifold is flat, the $F^{\mu\nu}$ field is massless, and the gauge group is $U(1)$. Close to particles the spacetime manifold is not flat, the $F^{\mu\nu}$ field may have mass, and the gauge group is $U(1) \times SU(2)$. This matches the electroweak unification [2–4].

D. Strong force

Quarks are linked $S^1 \times P^2$. No branch of M can intersect itself, therefore the quarks cannot unlink. This is quark confinement. When quarks are close to each other, the non-self-intersection constraint exerts no force. This is quark asymptotic freedom.

To describe the spacelike position of quarks within a hadron, we use 5-vectors. Label each quark q_n where the index n identifies the particular quark. Label the quark position vector q_n^j where j is the 5-vector index. Choose the origin of coordinates to be the center of the quarks so that $\sum_n q_n^j = 0$. The condition $|q_n^j| \leq 1$ for each q_n implies each quark must be within distance 1 of the center. Alternatively, add a sixth *non-physical* coordinate q_n^6 to each quark position vector and then require $|q_n^j| = 1$ for each n. The constraints $\sum_n q_n^j = 0$

and $|q_n^j| = 1$ for 6 dimensions and 3 quarks over-constrain by 1 degree of freedom, so we allow one q_n^5 to be variable. Convert the q_n^j vectors to complex 3-vectors, which we call the color charge.

$$(q_n^1, q_n^2, q_n^3, q_n^4, q_n^5, q_n^6) \to (q_n^1 + iq_n^2, q_n^3 + iq_n^4, q_n^5 + iq_n^6) \tag{11}$$

The quark position is irrelevant as long as the quarks are close enough. To disregard position we use a gauge group $SU(3)$ that maps between quark positions. However, the quark positions have 9 degrees of freedom, compared to the 8-dimensional group $SU(3)$. Although the group $SU(3)$ works as a gauge group, it is a subgroup of the group that maps between all quark positions. The color charge and $SU(3)$ gauge group match the QCD description of strong force [5–7].

E. Gravity

To descrive gravity, we separate the action $S[\Phi_M]$ into a component from matter and energy L_m and a component from the scalar curvature R.

$$S[\Phi_M] = \int w\big((1/2)F^{\mu\nu}F_{\mu\nu} - R\big)d\Phi_M = \int w(-R + L_m)d\Phi_M \tag{12}$$

For constant w, this is the Lagrangian of general relativity, which generates the same field equations. The spacetime manifold can carry momentum and energy in the form of a transverse wave. Therefore, considering the manifold in the 6-space allows for a description of gravitational field energy in $T^{\mu\nu}$ without requiring a pseudo-tensor.

To fully reproduce general relativity, we could ignore the geometry of Φ_M in the 6-space, describe its geometry with coordinate charts, apply the Lagrangian, and produce the same field equations on Φ_M. The result would imply a source term for curvature that is locally equivalent to $T^{\mu\nu}$ without the energy-momentum of gravity.

1. *Dark matter*

If w is not constant then it affects the gravitational Lagrangian. On small scales, w tends towards a uniform equilibrium distribution. On large scales, reaching a uniform equilibrium distribution takes longer. If the large-scale distribution of w on M is not uniform then the variations could affect spacetime curvature and appear as dark matter.

2. Geometry of gravity

If M is approximately flat then the optimal manifold Φ_M is $(x_0, x_1, x_2, x_3, f_1, f_2)$ where f_1 and f_2 are functions of the first 4 coordinates. If there are no masses and the boundary condition is flat, then $f_1 = f_2 = 0$. If there are masses, then the proper time $(1 - \beta^2)^{1/2}$ of those masses is reduced if they are in oscillatory motion and this improves the action $S[\Phi_M]$. The oscillation of those masses propagates standing waves in f_1 and f_2 that affect the geometry of M. This is the gravitational field. The two coordinates f_1 and f_2 have two degrees of freedom, which matches the degrees of freedom for a weak linear spin-2 field, as in general relativity.

3. Parity breaking in gravity

For a mass on the manifold, any kind of oscillatory motion improves the action $S[\Phi_M]$. The optimal oscillation is rotation. If there is no electromagnetic field then rotation is of the form $(x_0, x_1, x_2, x_3, bsin(k^\nu x_\nu), bcos(k^\nu x_\nu))$ for a causal vector field k^ν and amplitude b. There are two possible rotational directions. The action $S[\Phi_M]$ is optimized if the direction of rotation is the same everywhere on Φ_M. This is spontaneous parity breaking. The way that gravitational parity breaking produces neutrino helicity parity breaking is shown in the paper "Knot physics: neutrino helicity" [13].

VII. PROOFS

A. Entropy depends on $F^{\mu\nu}$ as $w \ln(1 + (1/2)F^{\mu\nu}F_{\mu\nu})$

The A^ν field represents displacement of the manifold. The A^ν field preserves causality on each branch B. On B, let $I^+(p)$ be the set of points in the future cone of p. Similarly let $I^-(p)$ be the set of points in the past of p. For a timelike vector t_ν, the set $A(t_\nu, p)$ is the points y sharing a branch with p such that $A^\nu(y)t_\nu = A^\nu(p)t_\nu$. We require that $A(t_\nu, p) \cap I^-(p) = \emptyset$ and $A(t_\nu, p) \cap I^+(p) = \emptyset$ for all p and all timelike t_ν. On a flat 2-manifold this implies

$|A^{0,1} - A^{1,0}| \leq 1$. On a n-manifold it implies $F^{\mu\nu} a_\mu F^\alpha_\nu a_\alpha \geq -1$ for all $|a_\mu| = 1$. Then $F^{\mu\nu} F_{\mu\nu} \geq -2$. Therefore $2 + F^{\mu\nu} F_{\mu\nu} \geq 0$. The density of virtual photons is linear in w, therefore the entropy is $w \ln(1 + (1/2) F^{\mu\nu} F_{\mu\nu})$.

Intuitively, the entropy is determined by the rate of quantum field oscillations. An electromagnetic field affects the rate of quantum field oscillations. If there is an electric field, then magnetic field oscillations are constrained because $\nabla \times E = -\partial B/\partial t$. A fast quantum magnetic field oscillation adds a large electric field, but the electric field strength is constrained by causality. Therefore a strong electric field restricts the speed of quantum magnetic field oscillations. The causal distance between two points is determined by the metric $h_{\mu\nu} = A_{\alpha,\mu} A^\alpha{}_{,\nu}$. An electric field reduces the causal distance between nearby points which reduces the quantum field oscillations. A magnetic field, however, increases the causal distance between nearby points. By the same reasoning, a magnetic field increases the rate of quantum field oscillations and therefore increases entropy.

B. Entropy depends on R as $w/(1 + R)$

Probability depends on branch interactions such that probability P is proportional to the number of branches coming into the interaction times the number of branches going out, as in section VI A. If we assume that the average number of branches in an interaction is k then the number of states associated with n consecutive interactions is k^n. For a density of branch interactions d, the density of states is k^d. The total branch weight w is much greater than the average number of branches k in an interaction. Many of the branch interactions are parallel and independent rather than consecutive. Therefore the number of states associated with branch weight w and independent branch interactions is $P = k^{dw}$. The Lagrangian is $L = \ln(P) = dw \ln(k)$.

The density of branch interactions d and the branch weight w are both affected by the scalar curvature R. The scalar curvature changes the volume of the manifold as $dV = (1 + R) dV_f$. The increase in volume reduces the branch weight w in proportion to the increase in volume. The total branch weight is conserved, $w = (w/(1 + R))(1 + R)$. However, the density of branch interactions is decreased to $d/(1 + R)$. If the volume of the manifold were increased to the limit, all of the weight w would be in a single branch of very large volume. Because that branch cannot interact with itself, the density of branch interaction would be zero, $d = 0$.

Using the formula for the Lagrangian in terms of branch interaction density d, we have $L = (d/(1+R))w\ln(k)$. Removing constants and linearizing in R this gives $L = w/(1+R)$ or $L \approx -wR$.

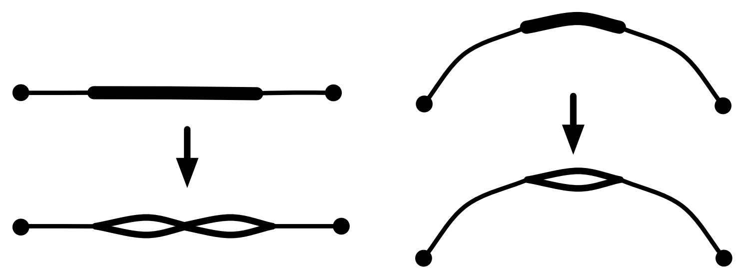

FIG. 17: Increasing the curvature R of Φ_M with a fixed boundary stretches the interior, which reduces the density of branching. Therefore entropy is maximized by minimizing the scalar curvature.

C. The homotopy constraints on a spacelike slice K of a branch B

Let B be a branch of the spacetime manifold M. Then, for a spacelike slice K of B, the homology groups $H_n(K)$ are constrained as follows.

1. $rank(H_0(K)) = 1$

The $rank(H_0(K)) = 1$. Assume that $H_0(K)$ changes. Then there is some slice K_t which is the last slice before $H_0(K)$ changes. Therefore there is some point on K_t where the tangent space is orthogonal to the time vector. This implies that the metric has signature $(0, 0, 4)$ and B is not a finite energy embedding.

2. $\pi_1(K)$ *is finite*

$\pi_1(K)$ must be finite. To show this, we show how $\pi_1(K)$ relates to the homotopy group $\pi_1(K_I)$ for an initial spacelike slice K_I. Let A be a submanifold in K_I. Then A can translate in B along a continuous causal vector field. For a particular vector field there is a translation τ and A maps to a set $\tau(A)$ in slice K_t. If τ translates A through surfaces that are unkinked then the topology of A never changes. This implies that $\pi_1(K_I)$ remains unchanged. However, if there is a kinked spacelike slice K_0 then we can imagine K_0 as a connecting piece between the homotopically trivial past K_I and a possibly homotopically non-trivial spacelike slice K. The translation τ may not be injective on K_0. If A is a S^1 then $\tau(S^1)$ may intersect itself so that it becomes multiple S^1 connected at a point. If A is a D^2 then intersections on the interior of $\tau(D^2)$ can be resolved by homotopy and $\tau(D^2)$ is still a D^2.

We want to find elements in $\pi_1(K)$ and determine what order those elements can have in $\pi_1(K)$. Let S be a S^1 in K. Then $S \subset \tau(S_I)$ for some τ and some S_I in the initial slice K_I. The initial slice K_I is homotopically trivial, therefore there is $D_I \subset K_I$, with D_I a D^2 such that S_I is the boundary of D_I (written $S_I = \partial D_I$). Then we translate D_I to $\tau(D_I)$. We have $S \subset \tau(S_I) = \tau(\partial D_I) = \partial(\tau(D_I))$. We can now translate all of the boundary of $\tau(D_I)$ onto S (a spacelike translation). For example we can move the boundary parallel to $\tau(D_I)$, at infinitesimal distance from it. The result is that m copies of S are the boundary of $\tau(D_I)$ for some finite m. Therefore S has order m or less in $\pi_1(K)$. Therefore $\pi_1(K)$ is finite.

3. $\pi_2(K)$ is non-trivial if the topology is non-trivial

If the topology of K is non-trivial then $\pi_2(K)$ must be non-trivial. To prove this, assume the topology of K is non-trivial but $\pi_2(K)$ is trivial. Without loss of generality, assume a constant topology for the constant time slices between the creation of the knot and the slice K. At the creation of the knot there is a set C where the metric is degenerate. Translate C forward along a continuous causal vector field with a mapping τ that maps to $\tau(C,t)$ in the constant time slice at time t with $\tau(C,t_0) = C$ at creation and $\tau(C,t_K)$ in K. If $\pi_2(K)$ is trivial then any 2-cycle in K is a 2-boundary. Any 2-boundary can be contracted to a 1-cycle without changing the manifold topology. Therefore B is topologically equivalent to a manifold B' in which $\tau(C,t)$ has been contracted to a 1-cycle for all t. However, a continuous causal vector field cannot diverge around a 1-dimensional metric degeneracy. Therefore there can be no topology change at $\tau(C,t_0)$. This implies the topology of K is trivial, which is a contradiction. Therefore a non-trivial topology on K implies a non-trivial $\pi_2(K)$.

D. $(S^1 \times P^2)_m$ **and** $(S^1 \times P^2)_n$ **have distinct embedding classes for** $m \neq n$

Let X and Y be 3-manifolds embedded in $\mathbb{R}^5$. The manifolds X and Y are the images of the following mappings:

$$\begin{aligned} &X : (r, \theta, \phi) \to (g(r), \theta, \phi, h(r)sin(2\theta + n\phi), h(r)cos(2\theta + n\phi)) \\ &Y : (r, \theta, \phi) \to (g(r), \theta, \phi, h(r)sin(2\theta + m\phi), h(r)cos(2\theta + m\phi)) \\ &g(r) = \begin{cases} 2r - 2 & \text{if } r < 2 \\ r & \text{otherwise} \end{cases} \qquad h(r) = \begin{cases} 2 - r & \text{if } r < 2 \\ 0 & \text{otherwise} \end{cases} \end{aligned} \tag{13}$$

with integers $m \neq n$. We want to prove that X and Y are distinct as embeddings, so we assume the opposite. Then there is an ambient isotopy $G : \mathbb{R}^5 \times I \to \mathbb{R}^5$ such that $G(\mathbb{R}^5, 0)$ is the identity mapping on $\mathbb{R}^5$ and $G(X, 1) = Y$. Let $X(\phi_0)$ be the subset of X with constant $\phi = \phi_0$ or $\phi = \phi_0 + \pi$. Let $X(r_1)$ and $Y(r_1)$ be the subsets of X and Y mapping from $r = 1$. Then $X(\phi_0)$ is topologically $\mathbb{R}^2 \# P^2 \# P^2$ and $G(X(\phi_0), 1)$ is also. This is true for any value of ϕ_0, therefore we can map those copies of P^2 onto each other such that the ambient isotopy G has an equivalent ambient isotopy G' with $G'(X(r_0), 1) = Y(r_0)$. Let R_0 be the subset of $\mathbb{R}^5$ with $r = 0$. Then with an ambient isotopy G' there is an equivalent ambient isotopy G'' with $G''(R_0, 1) = R_0$.

Let $X(\theta_0)$ and $Y(\theta_0)$ be the subsets of X and Y where $\theta = 0$ or $\theta = \pi$. Then $X(\theta_0)$ and $Y(\theta_0)$ are the 2-manifolds that intersect each $S^1 \times P^2$ along the S^1 fiber. The submanifolds $X(\theta_0)$ and $Y(\theta_0)$ are unique up to isotopy in X and Y, therefore there is an ambient isotopy G''' such that $G'''(X(\theta_0), 1) = Y(\theta_0)$.

Let $X(\theta_0, r_1)$ and $Y(\theta_0, r_1)$ be the subsets of X and Y that are the images of $(1, 0, \phi)$ in their respective mappings. Then $X(\theta_0, r_1) = X(\theta_0) \cap G'''(R_0, 0)$ and $Y(\theta_0, r_1) = Y(\theta_0) \cap G'''(R_0, 1)$. Therefore $G'''(X(\theta_0, r_1), 1) = Y(\theta_0, r_1)$.

Let C be the circle with $r = x_4 = x_5 = 0$. Then, as submanifolds of $G'''(R_0, 0)$ and $G'''(R_0, 1)$, the winding number of $X(\theta_0, r_1)$ around C is n and the winding number of $Y(\theta_0, r_0)$ around $G'''(C, 1)$ is m. However, G''' is an ambient isotopy on R_0, therefore the winding number should be preserved and there is a contradiction.

[1] E. C. Zeeman, Annals of Mathematics **78**, 501-526 (1963).

[2] S. Weinberg, Phys. Rev. Lett. **19**, 1264 (1967).

[3] A. Salam and J. Ward, Phys. Lett. **13**, 168 (1964).

[4] S. Glashow, L. Maiani, and J. Iliopoulos, Phys. Rev. D **2**, 1285 (1970).

[5] K. Wilson, Phys. Rev. D **10**, 2445 (1974).

[6] D. Gross and F. Wilczek, Phys. Rev. Lett. pp. 1343–1346 (1973).

[7] H. D. Politzer, Phys. Rev. Lett. pp. 1346–1349 (1973).

[8] C. Wall, Bull. Amer. Math. Soc. **71**, 564 (1965).

[9] R. Geroch, Journal of Mathematical Physics **8**, 782 (1967).

[10] W. B. R. Lickorish, Ann. of Math. **2**, 531 (1962).

[11] W. B. R. Lickorish, Proc. Cambridge Philos. Soc. **59**, 307 (1963).

[12] A. H. Wallace, Canad. J. Math. **12**, 503 (1960).

[13] C. Ellgen Knot physics: Neutrino helicity www.knotphysics.net

[14] C. Ellgen Knot physics: Deriving the fine structure constant www.knotphysics.net